

# POLYMER–DRUG NANOCONJUGATES

RONG TONG

*Department of Chemical Engineering, Massachusetts Institute of Technology, Cambridge, MA, USA Laboratory for Biomaterials and Drug Delivery, Department of Anesthesiology, Division of Critical Care Medicine, Children’s Hospital Boston, Harvard Medical School, Boston, MA, USA*

LI TANG, NATHAN P. GABRIELSON, QIAN YIN, AND JIANJUN CHENG

*Department of Materials Science and Engineering, University of Illinois at Urbana–Champaign, Urbana, IL, USA*

## 7.1 INTRODUCTION

Polymeric nanomedicine, an emerging field that involves the use of drug-containing polymeric nanoparticles (NPs) for cancer treatment, is expected to alter the landscape of oncology [1]. The medical application of nanotechnology has been extensive: roughly 40 nanomedicines have already been approved by the Food and Drug Administration (FDA) for clinical use [2–4] and a handful of NPs are currently in preclinical investigations [2,5]. Incorporation of chemotherapeutic agents in NP delivery vehicles can improve water solubility, reduce clearance, reduce drug resistance, and enhance therapeutic effectiveness [6]. Broadly speaking, two approaches have been used to load drugs in NPs for delivery. One is to encapsulate drugs within NPs via noncovalent bonds, that is, distribution of the drug throughout a polymeric matrix during formulation (Figure 7.1a) [7]. The second loading strategy is the formulation of NPs using polymer–drug conjugates, a technique first proposed in 1975 (Figure 7.1b) [8]. In this chapter, we discuss the pros and cons of the two strategies and introduce newly developed polymer–drug conjugates—so-called nanoconjugates—as a formulation strategy which addresses challenges faced by both encapsulates and conjugates

---

*Pharmaceutical Sciences Encyclopedia: Drug Discovery, Development, and Manufacturing*,  
Edited by Shayne C. Gad  
Copyright © 2013 John Wiley & Sons, Inc.

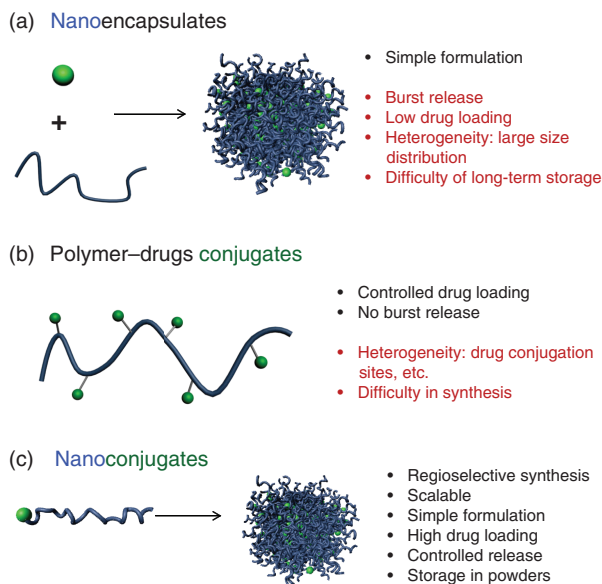


**FIGURE 7.1** Pros (black) and cons (gray) of (a) nanoencapsulates (NEs) and (b) polymer–drug conjugates. We propose (c) nanoconjugates (NCs) with reduced heterogeneity to address the challenges in both encapsulated and conjugated systems.

(Figure 7.1c). Along the way, we also discuss topics related to regioselective polymer–drug conjugation chemistry, *in vitro* formulation and characterization, and present preliminary *in vivo* studies that highlight the potential clinical translation of nanoconjugates.

## 7.2 CURRENT STATUS OF NANOENCAPSULATES AND POLYMER–DRUG CONJUGATES

### 7.2.1 Nanoencapsulates

Nanoparticles loaded with a drug via encapsulation within a polymer matrix are termed nanoencapsulates. Although nanoencapsulate formulation is straightforward in both concept and fabrication, their clinical use is challenged by a variety of issues (Figure 7.1a). First, nanoencapsulates often show “burst” drug release profiles in aqueous solution, with as much as 80–90% of the encapsulated drug released during the first few to tens of hours [9]. The rapid drug release, also called dose dumping, can prevent the drug from operating within its therapeutic window and cause severe systemic toxicity [10]. Second, drug loading in nanoencapsulates is very low—typically in the range of 1–5% for most NPs studied—and is widely variable depending on the amount of drug being used, the hydrophobicity/hydrophilicity of the drug as well as the compatibility between the drug and the polymer [9, 11]. Drug loading, in particular, is a critical measure of the feasibility of nanoencapsulate delivery systems in clinical

settings [11]. At low drug loading, large amounts of delivery vehicles are needed to achieve therapeutic concentrations. However, because of the limited body weight and blood volume of animals, administration volumes are fixed. For mice with 20–30 g body weight, the intravenously injected volume must be kept around 100–200  $\mu\text{L}$  [12]. Thus, the intravenous administration of NPs with 1% drug loading in a 100  $\mu\text{L}$  solution at a dose of 50 mg/kg (e.g., docetaxel) would require a 1 g/mL NP solution. In practice, it is impossible to formulate such concentrated solutions and inject them intravenously. Another problem related to drug loading is the lack of a general strategy to achieve quantitative drug encapsulation in many NPs (e.g., polylactide (PLA) and poly(lactic-co-glycolic acid) (PLGA) NPs). In this instance, nonencapsulated drugs may self-aggregate, thus complicating their removal from the NPs [13]. Ultimately, these formulation challenges significantly impact the processability and the clinical translation of nanoencapsulate delivery vehicles for cancer therapy.

## 7.2.2 Polymer-Drug Conjugates

As difficulties facing nanoencapsulate drug loading began emerging, considerable interest was shifted to drug delivery strategies employing polymer-drug conjugates (Figure 7.1b). In fact, a polymer-protein drug conjugate has already been approved for use in Japan, and a handful of other polymer-drug conjugates are presently transitioning from later clinical trials to the wider market [10,14]. One of the first systems explored, *N*-(2-hydroxypropyl)methacrylamine (HPMA) polymer-drug conjugates developed by Duncan and Kopecek in the late 1970s, has led to various clinical trial candidates [14,15]. Other interesting types of polymer-drug conjugates include cyclodextrin-containing polymers with conjugated camptothecin developed by Davis laboratory (IT-101) [16–20] and dendritic polyester-drug conjugates developed by Frechet and coworkers [21,22].

One of the primary challenges facing polymer-drug conjugate delivery systems is the actual conjugation step. Not only does the conjugation often require extensive post-conjugation purification steps, the heterogeneity of polymer-drug conjugates arising from nonsite-specific coupling reactions may also present bottlenecks to the clinical translation [10]. As shown in Figure 7.2, heterogeneities of polymer-drug conjugates result from (1) molecular weight distributions (MWDs, Mw/Mn) of the polymers (Figure 7.2a), (2) lack of control of the drug conjugation site on the polymer backbone (Figure 7.2b), and (3) lack of regioselectivity with regard to the conjugation site on drugs with multiple conjugation-amenable functional groups (Figure 7.2c). This last point is particularly relevant, as many of the best-selling anticancer small molecule drugs (e.g., paclitaxel, docetaxel, and doxorubicin) contain multiple functional groups (e.g., multihydroxyl groups in all three agents; ketone and amine groups in doxorubicin) for conjugation [23]. In the past several decades, there have been numerous efforts to minimize heterogeneities within polymer-drug conjugates. These include the development of polymers with low MWDs (e.g., dendrimers) [22,24–31], the conjugation of therapeutic agents to specific sites along the polymer backbone (e.g., the termini) [16,32–38], and the activation of specific functional groups on the therapeutic agents by means of

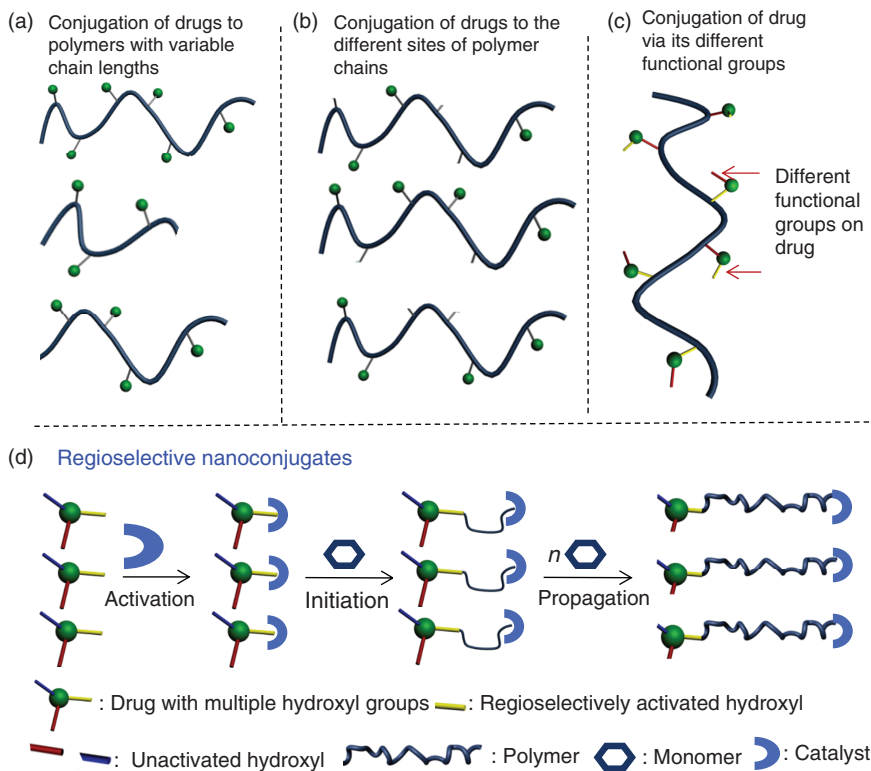


**FIGURE 7.2** Heterogeneities in polymer-drug conjugates: (a) polymer–drug conjugates with a broad distribution of polymer chain lengths; (b) polymer–drug conjugates in which the conjugation site on the polymer backbone is uncontrolled; (c) polymer–drug conjugates in which a multifunctional therapeutic agent is conjugated without regioselectivity. Our solution to the heterogeneity problem: (d) drug-initiated, controlled polymerization for the synthesis of polymer–drug conjugates with low MWDs; the drug molecules are conjugated regioselectively to the polymer termini.

protection/deprotection chemistry [39,40]. However, concise synthetic strategies that yield polymer–drug conjugates with minimal heterogeneity for clinical application are still lacking (Figure 7.2a–c).

## 7.3 NANOCONJUGATES: DESIGN AND SYNTHESIS

### 7.3.1 Design and General Consideration

We present here a new synthetic strategy to address challenges faced by both nanoencapsulates and polymer–drug conjugates. In particular, we focus on chemistry that allows for site-specific conjugation of a drug to a polymer with a narrow molecular weight distribution (MWD) with quantitative incorporation efficiency.

In designing such a synthetic strategy, we first considered chemical systems which already benefit from controlled and precise chemistry, like the well-established and controlled polymerization methodologies allowing for the preparation of polyesters [41,42], polypeptides [43,44], and hydrocarbon-based synthetic biopolymers [45] with precisely controlled molecular weights (MWs) and narrow MWD. By incorporating these existing strategies in our design, polymer–drug conjugates can be produced with precise and homogeneous chemical structure and, ultimately, improved performance.

Ring-opening polymerization (ROP) for the preparation of PLA polyesters has been investigated extensively [46,47]. The polymerization reaction typically involves lactide (LA) ring opening by a metal–alkoxide ( $L_nM-OR$ ) to form a RO-terminated LA–metal alkoxide ( $ROOCCH(CH_3)O-ML_n$ ) followed by chain propagation to form RO-terminated PLA [41,46,47]. According to this mechanism, the RO group ultimately is connected to the PLA terminus through an ester bond (Figure 7.3a). This process is well understood and has been used extensively for the

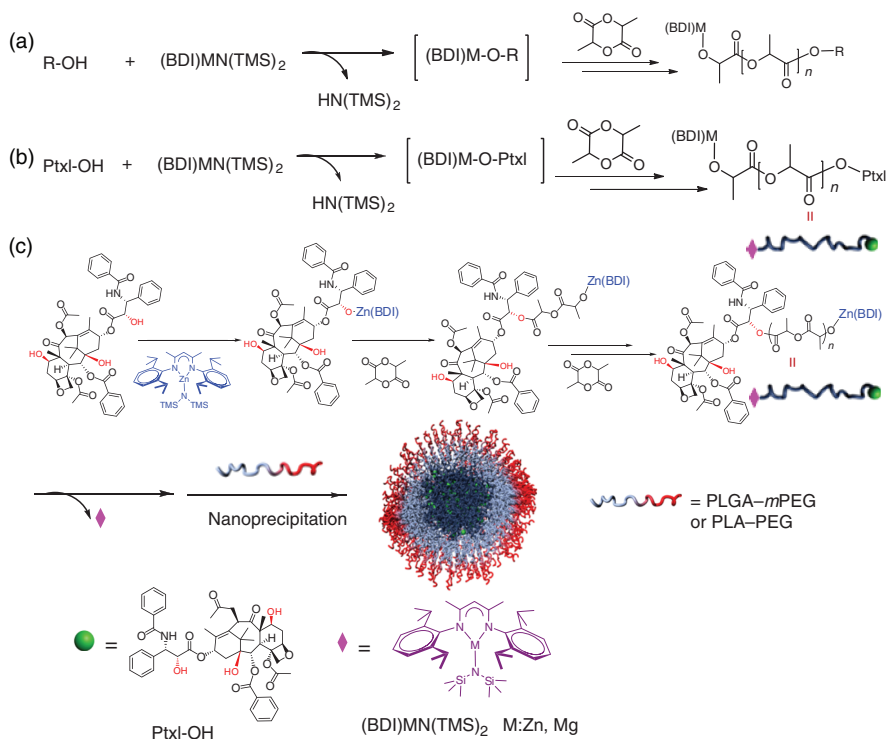


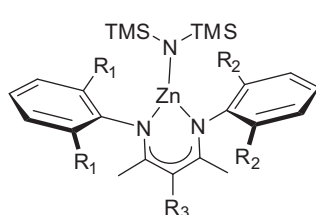
**FIGURE 7.3** (a) Mechanism of ROP of PLA initiated by R-OH/BDI-metal catalyst. We propose the mechanism can be applied to (b) complex molecules with dense hydroxyl groups, for example, Ptxl, to initiate ROP. (c) Regioselective coordination of (BDI-II)ZnN(TMS)<sub>2</sub> onto 2'-OH of Ptxl to initiate ROP of LA. The polymers can be nanoprecipitated with PLGA-mPEG or PLA-mPEG to formulate sub-120 nm NPs.

incorporation of hydroxyl-containing small molecules [38], macromolecules [48], and NPs [49] to the termini of PLA.

In the context of delivery technology, hydroxyl groups of drugs can be utilized to achieve controlled living polymerization of LA. The hydroxyl group is the most abundant functional group in natural products, being found in about 65% of the ~78,000 known pharmacophores as well as in several of the best-selling anticancer small molecule drugs. Thus, the active initiator for PLA polymerization can be prepared *in situ* by mixing a hydroxyl(s)-containing drug with an active metal complex, such as a metal-amido [41,50]. If well designed, the *in situ* formed M-ORs can initiate controlled polymerization of LA, resulting in quantitative incorporation of OR with 100% monomer conversion (Figure 7.3b) [41,46]. By judicious control of the metal catalyst ligand, it is also possible to control the regioselective coordination of a structurally complex drug molecule bearing multiple hydroxyl groups (Figure 7.2d). After ROP, the linear PLA will be covalently linked onto the specific hydroxyl group of the drug via an ester bond. PLA-drug conjugates can then be driven to form NPs—called nanoconjugates (NCs)—by nanoprecipitation methods (Figure 7.3c). Unlike nanoencapsulates, the use of a degradable ester linkage between a drug and a polymer prevents burst release from the NPs and facilitates the controlled release of drugs from the conjugates.

ROP of LA to generate polymer-drug conjugates with precise and homogenous chemistry has been examined in several studies performed by the Cheng laboratory [10,51,52]. For these studies, the ROP of LA was catalyzed by (BDI-X)Mn(TMS)<sub>2</sub> (BDI = 2-((2,6-dialkylphenyl)amino)-4-((2,6-dialkylphenyl)imino)-2-pentene, M = Mg or Zn, Table 7.1), a class of catalysts developed by Coates and coworkers for the controlled ROP of LA [41,50]. The strategy allows for quantitative incorporation of multihydroxyl drugs [51] (e.g., paclitaxel (Ptx1), docetaxel (Dtx1), and doxorubicin (Doxo)), other hydroxyl-containing therapeutic molecules [52] (e.g., camptothecin (Cpt), cyanine, cyclopamine) and even small peptides (goserelin) via ester bonds. By tuning the substituents on the *N*-aryl groups (R<sub>1</sub> and R<sub>2</sub>) and the β-position (R<sub>3</sub>) of

**TABLE 7.1 (BDI-X)ZnN(TMS)<sub>2</sub> for NCs Synthesis**

	Ligand	R <sub>1</sub>	R <sub>2</sub>	R <sub>3</sub>
	BDI-II	<i>i</i> Pr	<i>i</i> Pr	H
	(BDI-X)ZnN(TMS) <sub>2</sub>			
	BDI-EE	Et	Et	H
	BDI-EI	Et	<i>i</i> Pr	H
	BDI-IICN	<i>i</i> Pr	<i>i</i> Pr	CN

the BDI ligand (Table 7.1) [53], regioselective polymerization on specific hydroxyl groups can be achieved (Table 7.2). The controlled polymerization also can be expanded to other biopolymers, such as poly( $\delta$ -valerolactone), poly(trimethylene carbonate), and poly( $\epsilon$ -caprolactone) (Table 7.3 for various polymers loaded with PtxI and DtxI). Apart from their controlled chemistry, drug-PLA conjugates can be nanoprecipitated to generate NPs with sub-120 nm diameter, high drug loading, nearly quantitative loading efficiencies, controlled release profiles without burst release, and narrow particle size distributions [51,52,54,55].

The controlled chemistry mentioned earlier was validated in the synthesis of PtxI-PLA, and Doxo-PLA NCs. In the following discussion of these NCs, we examine the catalyst metal selection to achieve selective activation of hydroxyls in Cpt without disrupting the lactone ring structure [54]. Regioselective polymerization chemistry is also explored in the synthesis of PtxI-PLA and Doxo-PLA NCs, whose initiator drugs possess multiple hydroxyl groups as well as other functional moieties. Combined, these experiments demonstrate that the proposed NC synthetic strategy is widely applicable for the synthesis of drug-polymer conjugates with various hydroxyl-containing therapeutics and with various polymer backbones.

### 7.3.2 Synthesis of Cpt-PLA Nanoconjugates

20(*S*)-Camptothecin (Cpt), a topoisomerase I inhibitor isolated from the Chinese tree *Camptotheca acuminata*, exhibits a broad range of anticancer activity in various animal models [56,57]. In terms of usability, Cpt has low aqueous solubility in its therapeutically active lactone form and is transformed rapidly to its carboxylate analog at physiological pH, producing a highly toxic and therapeutically inactive molecule (Figure 7.4a) [58,59]. While Cpt-polymer conjugates have been prepared to overcome the solubility limitation of the drug, conjugates prepared with conventional coupling chemistry are plagued by various heterogeneities. For example, experiments exploring the conjugation of Cpt via condensation reactions yield MWDs over a range 1.5–2.5 [16]. Meanwhile, direct conjugation of Cpt through its C20-tertiary hydroxyl is a difficult multistep reaction: Cpt must first be converted to a Cpt-amino ester and then conjugated to a polymer containing carboxylate groups via the amine end group of the Cpt-amino ester [16,60]. If the polymer has pendant functional groups, Cpt conjugation is further complicated.

To synthesize Cpt-PLA NCs via ROP, we first explored its ability to form Cpt-metal complexes with various BDI catalysts. When mixed with (BDI-II)MgN(TMS)<sub>2</sub>, the C20-OH of Cpt formed a (BDI-II)Mg-Cpt alkoxide *in situ*. ROP of LA with this complex resulted in 100% LA conversion. HPLC analysis showed that Cpt was entirely conjugated to PLA with no detectable free Cpt in the polymerization solution. Although the  $M_n$  of the resulting polymer was in good agreement with the expected  $M_n$ , the MWD of Cpt-LA<sub>100</sub> was relatively broad (1.31) due in part to chain transfer during polymerization [41]. In order to achieve a better controlled polymerization, we next tested (BDI-II)ZnN(TMS)<sub>2</sub>. However, the (BDI-II)ZnN(TMS)<sub>2</sub>/Cpt-mediated ROP resulted in only 61% Cpt incorporation, indicating inefficient formation of Cpt-Zn complexes during the initiation step (Table 7.4)

**TABLE 7.2 Formulation of NCs with Hydroxyl-Containing Therapeutic and Dye Molecules<sup>a</sup>**

Drug	[LA]/[Drug]	NCs	Loading (wt%)	LA Conversion (%)	Loading Efficiency (%)	Size (nm)	PDI	Reference
		<b>Paclitaxel (Ptxl)</b> Mitotic inhibitor						
		<b>Docetaxel (Dtxl)</b> Mitotic inhibitor						
		<b>Camptothecin (Cpt)</b> Topoisomerase I inhibitor						
		<b>Doxorubicin (Doxo)</b> Intercalating DNA, topoisomerase II inhibitor						
		<b>Cyclopamine (Cpa)</b> Hedgehog pathway inhibitor						
		<b>Cy5-OH (Cy5)</b> Fluorescent molecule						
		<b>Goserelin (Gos)</b> Gonadotropin releasing hormone agonist						
Cpt	10	Cpt-LA <sub>10</sub>	19.5	>99	>99	72.5 ± 0.7	0.06 ± 0.02	[54]
Ptxl	25	Ptxl-LA <sub>25</sub>	19.2	>99	97	55.6 ± 0.5	0.04 ± 0.01	[51]
Ptxl	15	Ptxl-LA <sub>15</sub>	28.3	>99	95	85.5 ± 1.4	0.09 ± 0.03	[51]
Dtxl	10	Dtxl-LA <sub>10</sub>	35.9	>99	97	77.9 ± 1.5	0.06 ± 0.02	[51]
Doxo	25	Doxo-LA <sub>25</sub>	13.1	>99	98	90.8 ± 0.9	0.09 ± 0.01	[52]
Doxo	10	Doxo-LA <sub>10</sub>	27.4	>99	94	125.2 ± 2.3	0.11 ± 0.01	[52]
Cpa	50	Cpa-LA <sub>50</sub>	5.4	>99	>99	78.0 ± 2.4	0.12 ± 0.01	[52]
Cy5	25	Cy5-LA <sub>25</sub>	12.3	>99	>99	76.3 ± 3.8	0.06 ± 0.01	[52]
Gos	10	Cy5-LA <sub>10</sub>	46.8	>99	>99	120.6 ± 2.7	0.01 ± 0.01	[52]

LA, lactide; NCs, nanoconjugates; PDI, polydispersity.

<sup>a</sup>In molecule structures, the hydroxyl groups are differentiated in dark gray (regioselective conjugated to NCs) and in light gray. The functional group competing with hydroxyl groups (i.e., amine) is labeled in lightest gray.



**TABLE 7.3 Ptxl (or Dtxl)/(BDI-II)/ZnN(TMS)<sub>2</sub>-Mediated ROP of LA, VL, CL, and TMC**

Initiator (R)	Monomer	[M]/[R]	Time	Temperature (°C)	Conversion (%)	Incorporation efficiency (%)	$M_p/M_{exp}$ ( $\times 10^3$ g/mol)	MWD ( $M_w/M_n$ )
Ptxl	LA	200	12	r.t.	>99	>99	29.7/28.1	1.02
Ptxl	VL	100	12	r.t.	>99	>99	15.1/10.8	1.17
Ptxl	CL	200	10	r.t.	>99	>99	20.3/23.7	1.07
Ptxl	TMC	100	6	50	>99	>99	14.7/11.1	1.10
Dtxl	LA	200	12	r.t.	>99	>99	29.6/25.2	1.03
Dtxl	CL	100	10	r.t.	>99	>99	11.2/12.2	1.05
Dtxl	TMC	200	6	50	>99	>99	25.9/21.3	1.19
Dtxl	VL	100	12	r.t.	>99	>99	14.2/10.7	1.15

M, monomer;  $M_{exp}$ , expected molecular weight; MWD, molecular weight distribution; r.t., room temperature.

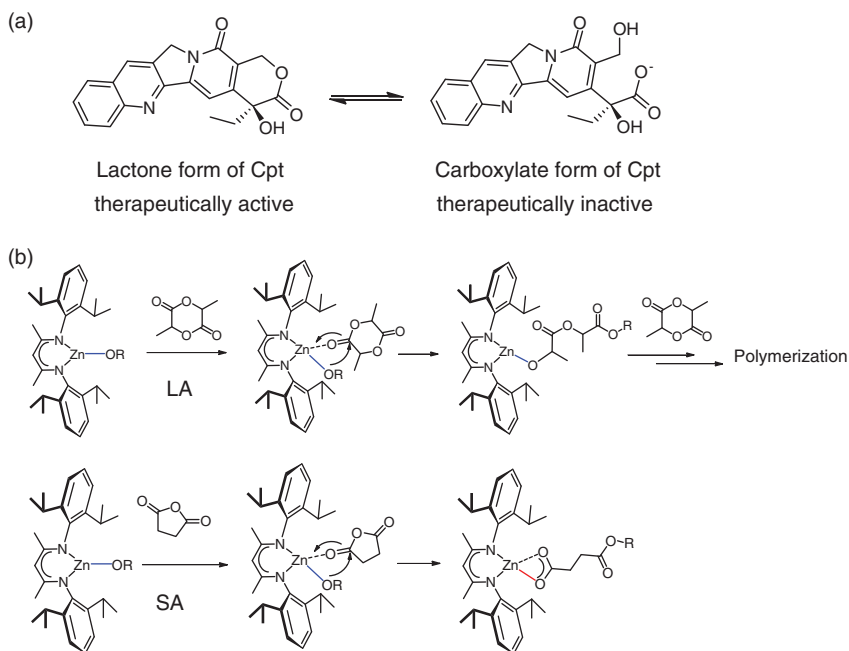


**FIGURE 7.4** (a) Equilibrium of Cpt Lactone and carboxylate forms. (b) Suggested insertion-coordination mechanism of (BDI)Zn-OR mediated ring-opening of lactide (LA) and succinic anhydride (SA). R group represents the PLA polymer chain or agents containing hydroxyl group(s) (e.g., Cpt).

[54]. The insufficient activation of the C20-OH of Cpt by (BDI-X)Zn was addressed by subtly tuning the 2- and 6-substituents of the *N*-aryl groups on the catalyst. Doing so, 100% incorporation efficiencies were observed in both (BDI-EE)ZnN(TMS)<sub>2</sub>/Cpt- and (BDI-EI)ZnN(TMS)<sub>2</sub>/Cpt-mediated polymerizations (Table 7.4) [54].

**TABLE 7.4** Ring Opening Reaction of SA and Polymerization of LA, Mediated by Cpt- (BDI-X)MN(TMS)<sub>2</sub> (M=Mg or Zn)<sup>a</sup>

Catalyst	Cpt loading efficiency (%)	Polymer MWD	Cpt-SA (%)	Cpt-Carboxylate <sup>a</sup>
(BDI-II)MgN(TMS) <sub>2</sub>	>99	>1.3	78	Yes
(BDI-II)ZnN(TMS) <sub>2</sub>	61	<1.1	19	Yes
(BDI-EE)ZnN(TMS) <sub>2</sub>	>99	>1.2	N.D.	N.D.
(BDI-EI)ZnN(TMS) <sub>2</sub>	>99	~1.1	89	No

MWD, molecular weight distribution.

<sup>a</sup>Determined by HPLC analysis of Cpt-SA reaction mediated by different metal catalysts. The Cpt-carboxylate form indicated that the catalyst might have deleterious effect toward Cpt.

In addition to concerns regarding the ROP of LA, we also examined the retention of the lactone ring of Cpt throughout polymerization. As mentioned earlier, the lactone ring of Cpt is unstable and subject to ring opening in the presence of a nucleophile. To ensure that the therapeutically active form of Cpt is released in physiological conditions, the lactone ring of the drug must be maintained throughout the conjugation reaction. As LA is subject to rapid polymerization and the resulting Cpt-PLA conjugate is difficult to be characterized precisely, we used succinic anhydride (SA) as a model monomer to study (BDI-X)ZnN(TMS)<sub>2</sub>/Cpt-mediated initiation. The ring opening of SA follows the same coordination-insertion mechanism as the initiation step of LA ROP but does not involve the subsequent chain propagation. Thus, the resulting product, Cpt-succinic acid (Cpt-SA), is a small molecule instead of a polymer. As a small molecule, the structure of Cpt-SA can be determined by routine characterization methods (Figure 7.4b). Experiments with SA revealed that Cpt activation by (BDI-II)MgN(TMS)<sub>2</sub> resulted in Cpt lactone ring opening (Table 7.4) [54]. The catalyst (BDI-EI)ZnN(TMS)<sub>2</sub>, however, was able to prevent Cpt carboxylate formation. Using this catalyst, controlled polymerizations were observed over a broad range of LA/Cpt ratios from 75 to 400 in excellent agreement with the expected MWs and with narrow MWDs (1.02–1.18) [54].

With enhanced polymerization chemistry, Cpt-PLA NCs have improved formulation properties. Because both monomer conversion and drug incorporation are quantitative in Cpt-PLA synthesis, drug loadings can be predetermined by adjusting LA/Cpt feeding ratios. At a low monomer/initiator (M/I) ratio of 10, the drug loading can be as high as 19.5% (Cpt-LA<sub>10</sub>, Table 7.2). To our knowledge, this Cpt-PLA NC has one of the highest loadings of Cpt ever reported [54]. Even at this high drug loading, sustained release of Cpt from Cpt-LA<sub>10</sub> NC was observed through the hydrolysis of the ester linker that connects the Cpt and the PLA without any observed burst release. Furthermore, the released Cpt (in PBS) had an HPLC elution time identical to authentic Cpt and was confirmed to have an identical molecular structure after isolation and characterization by <sup>1</sup>H NMR [54]. In contrast, PLA/Cpt NPs prepared by co-precipitation have been previously reported to give low drug loading (0.1–1.5%), low loading efficiency (2.8–38.3%), and poorly controlled release kinetics (20–90% of the encapsulated Cpt released within 1 h in PBS) [61]. Our unique conjugation technique allows for formation of Cpt-containing PLA NCs with superbly controlled formulation parameters, thus making Cpt-PLA NCs potentially useful agents for sustained treatment of cancer *in vivo*.

### 7.3.3 Synthesis of Ptxl-PLA (Dtxl-PLA) Nanoconjugates

Initially isolated from the bark of the yew tree, Ptxl is a potent anticancer drug that was originally used as a treatment for ovarian and breast cancer. Its use has since expanded and the drug is now also used to treat lung, liver, and other types of cancer. Clinical application of Ptxl is often accompanied with severe, undesirable side effects partially due to the solvent Cremophor EL in the commercial formulation of Taxol<sup>TM</sup>. To reduce the side effects, various nanoparticulate delivery vehicles have been developed and investigated in the past few decades [62–65], including

the FDA-approved albumin-bound Ptxl NPs (Abraxane<sup>TM</sup>). Ptxl's analog, Dtxl (Taxotere<sup>TM</sup>), is currently one of the best-selling chemotherapeutic agents and is used in the treatment of breast, ovarian, prostate, and nonsmall cell lung cancer. Many current NP formulations of both taxanes typically have low drug loadings, uncontrolled encapsulation efficiencies, and significant drug burst release effects when used *in vivo* [10,13,66,67]. Adding to formulation troubles, the densely functionalized structures of both molecules make it difficult to produce homogeneous Ptxl- and Dtxl-polymer conjugates.

Ptxl has three hydroxyl groups at its C2', C1, and C7 positions which can initiate LA polymerization, resulting in Ptxl-PLA conjugates with 1-3 PLA chains attached (Figure 7.5a). The three hydroxyl groups differ in steric hindrance in the order of 2'-OH < 7-OH < 1-OH. The tertiary 1-OH is least accessible and is typically inactive [68]. The 7-OH, however, can potentially compete with 2'-OH [69] for coordination with metal catalysts. In order to differentiate the initiation site between the two hydroxyl groups, we postulated that a metal catalyst with a bulky chelating ligand would preferentially form Ptxl-metal complexes through the 2'-OH for site-specific LA polymerization.

A selective reduction reaction was used to divide Ptxl into two fragments—one with the 2'-OH and the other with the 1- and 7-OHs—in order to study the impact of catalyst on regioselectivity [70]. Tetrabutylammonium borohydride (Bu<sub>4</sub>NBH<sub>4</sub>) can selectively and quantitatively reduce the C13-ester bond of Ptxl to produce baccatin III (BAC) and (1*S*,2*R*)-*N*-1-(1-phenyl-2,3-dihydroxypropyl)benzamide (PDB; Figure 7.5a) [70]. Thus, Ptxl-LA<sub>5</sub> was generated using a variety of catalysts, reduced with Bu<sub>4</sub>NBH<sub>4</sub> and examined using HPLC-MS analysis. Doing so, we found that Mg(N(TMS)<sub>2</sub>)<sub>2</sub>—a catalyst without a chelating ligand—initiates polymerization non-preferentially at both the 2'-OH and the 7-OH. Its counterpart with a bulky BDI-II ligand (e.g., (BDI-II)MgN(TMS)<sub>2</sub>) preferentially initiates polymerization at the 2'-OH position. However, the resulting Ptxl-PLAs displayed fairly broad MWD (>1.2). We reasoned that the observation was attributable to fast propagation relative to initiation for the Mg catalysts [41]. Thus, to reduce the MWD of polymers, we utilized a zinc analog, (BDI-II)ZnN(TMS)<sub>2</sub>, to give a more controlled LA polymerization with a narrow MWD (1.02, Figure 7.5b) [41].

We further examined the effect of the ligand on initiation regioselectivity and LA polymerization by (BDI-X)ZnN(TMS)<sub>2</sub>/Ptxl by varying the steric bulk of the *N*-aryl substituents (R<sub>1</sub> and R<sub>2</sub>) and the electronic properties of R<sub>3</sub> (Table 7.5) [41,53,71,72]. While both PDB-PLA and BAC-PLA are observed for Ptxl-LA<sub>5</sub> initiated by (BDI-EE)ZnN(TMS)<sub>2</sub>/Ptxl, analysis of the fragments of the reductive cleavage of (BDI-EI)ZnN(TMS)<sub>2</sub>/Ptxl showed relatively reduced amounts of BAC-PLA. This indicates that a Zn catalyst with bulky *N*-aryl substituents will preferentially coordinate with the 2'-OH of Ptxl to initiate PLA polymerization. Of note, various studies suggest that the polymerization process does not lead to deleterious effect on Ptxl—the Ptxl can be loaded and released with intact structure.

SA was again used as a model monomer to study the initiation step of ROP. Such reactions yield a small molecule, Ptxl-succinic acid (Ptxl-SA), whose structure can be determined easily by routine characterization methods (Table 7.5). The results

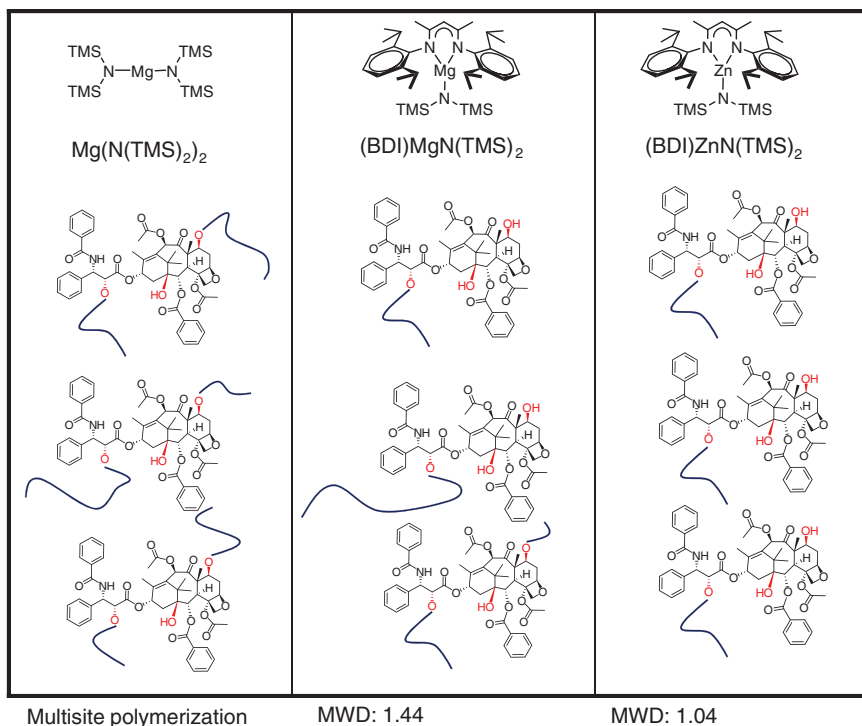
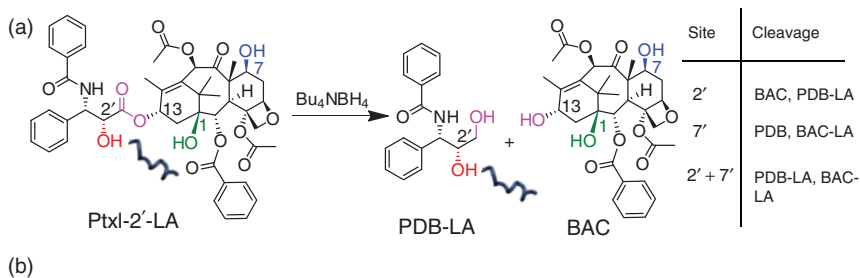


**FIGURE 7.5** (a)  $\text{Bu}_4\text{NBH}_4$ -induced site-specific degradation of Ptxl for the formation of PDB and baccatin (BAC). (b) Scheme of Ptxl-PLA conjugates mediated by different catalysts, with the indication of regioselectivity and molecular weight distributions (MWDs).

show that the regioselectivity of the Ptxl/SA reaction increases as the sizes of  $\text{R}_1$  and  $\text{R}_2$  increase, in good agreement with the reductive reaction study using  $\text{Bu}_4\text{NBH}_4$ . The catalyst  $(\text{BDI-II})\text{ZnN}(\text{TMS})_2$  showed the best regioselectivity while  $(\text{BDI-EE})\text{ZnN}(\text{TMS})_2$  showed the worst. Changing  $\text{R}_3$  from  $-\text{H}$  (BDI-II) to the electron-withdrawing  $-\text{CN}$  group (BDI-IICN) did not change the regioselectivity of the Ptxl/SA reaction. However, the addition of the CN group enhanced the reactivity of the resulting catalyst  $(\text{BDI-IICN})\text{ZnN}(\text{TMS})_2$ , leading to a higher yield of Ptxl-2'-SA (Table 7.5). Controlled polymerization of PLA was observed when  $(\text{BDI-II})\text{ZnN}$

**TABLE 7.5 Regioselectivity of the Ptxl/Metal Catalyst-Mediated Ring Opening Reactions**

Catalyst	Reduction of Ptxl-LA <sup>a</sup>	Ptxl-2'-SA (%)	Regioselectivity <sup>a</sup>	Regioselectivity for 2'-OH <sup>b</sup>	Polymer MWD
Mg[N(TMS) <sub>2</sub> ] <sub>2</sub>	PDB-LA, BAC-LA	N.D.	2'-OH and 7-OH	N.D.	>1.4
(BDI-ID)MgN(TMS) <sub>2</sub>	Majority PDB-LA, BAC	N.D.	Majority 2'-OH	N.D.	>1.4
(BDI-ID)ZnN(TMS) <sub>2</sub>	PDB-LA, BAC	40	2'-OH	100	<1.1
(BDI-EE)ZnN(TMS) <sub>2</sub>	PDB-LA, BAC-LA	30	2'-OH and 7-OH	35	1.3
(BDI-EI)ZnN(TMS) <sub>2</sub>	Majority PDB-LA, BAC	45	Majority 2'-OH	77	~1.2
(BDI-IICN)ZnN(TMS) <sub>2</sub>	PDB-LA, BAC	54	2'-OH	100	<1.1

<sup>a</sup>Determined by HPLC analysis of Ptxl-LA<sub>5</sub> site-specific reduced by Bu<sub>4</sub>NBH<sub>4</sub>.

<sup>b</sup>Determined by HPLC analysis of Ptxl-SA ring opening reactions mediated by (BDI-X)Zn catalyst.

(TMS)<sub>2</sub>/Ptxl was used at various [LA]/[Ptxl] ratios (50/1–300/1), with the obtained MWs in excellent agreement with the expected MWs and the monomodal MWDs in the range of 1.02–1.09.

Dtxl, the Ptxl analog, has four hydroxyl groups at C2', C1, C7, and C10 (Table 7.2). To examine the regioselectivity of Dtxl-initiated ROP of LA, we examined the Dtxl/(BDI-X)ZnN(TMS)<sub>2</sub>-mediated ring opening reaction of SA. When complexed with (BDI-II)ZnN(TMS)<sub>2</sub>, Dtxl reacted with SA to yield Dtxl-2'-SA with 100% regioselectivity and 71.5% yield. (BDI-II)ZnN(TMS)<sub>2</sub>/Dtxl also showed excellent control for the ROP of LA, affording Dtxl-PLA with predictable MWs and very narrow MWDs. NCs formed with either Ptxl-PLA or Dtxl-PLA showed unprecedented high loading—up to 28.3 wt% in Ptxl-LA NCs and up to 35.9 wt% in Dtxl-LA NCs. The detailed formulation methods and efficacy of both conjugates are further discussed in Section 7.4.

Poly( $\delta$ -valerolactone) (PVL), poly(trimethylene carbonate) (PTMC), and poly( $\epsilon$ -caprolactone) (PCL) have been used extensively as alternatives to PLA in suturing, drug delivery, and tissue engineering applications. We were therefore interested as to whether the Ptxl (or Dtxl)/(BDI-II)ZnN(TMS)<sub>2</sub>-mediated ROP of LA could be extended to the synthesis of Ptxl-PCL, Ptxl-PVL, and Ptxl-PTMC conjugates. Ptxl/(BDI-II)ZnN(TMS)<sub>2</sub> showed excellent control over the polymerization of  $\delta$ -valerolactone (VL), trimethylene carbonate (TMC), and  $\epsilon$ -caprolactone (CL). All the polymerization reactions gave drug-polymer conjugates with the expected MWs and narrow MWDs ( $M_w/M_n < 1.2$ ) (Table 7.3). Furthermore, the polymerizations of VL and CL proceeded at room temperature, and the monomer conversions were quantitative. The polymerization of TMC, however, required a slightly elevated reaction temperature (6 h at 50°C).

### 7.3.4 Synthesis of Doxo-PLA Nanoconjugates

Doxo is commonly used in the treatment of a wide range of cancers and leukemia. Clinically, Doxo is administered as Doxil<sup>TM</sup>, a PEGylated liposome-encapsulated form of the drug [74,75]. Owing to its high hydrophilicity, the encapsulation of Doxo within a hydrophobic polymer matrix can be challenging. For micelles formed by coprecipitating Doxo and PLGA-PEG, reported values indicate Doxo loading and loading efficiency as low as 0.51% and 23%, respectively [76]. Doxo loadings of 0.6–8.7% with loading efficiencies of 11.4–43.6% have also been reported by Hubbell and coworkers in their encapsulation studies using inverse emulsion polymerization of nonprotonated Doxo [77]. However, even with techniques allowing increased loading, burst release of Doxo is reported in many NP delivery systems [40,76,77].

Conjugation of Doxo to polymers can be difficult due to the diverse functional groups presented by the drug. Doxo has three hydroxyl groups, two phenolic hydroxyls, one ketone group, and one amine group. Doxo is also sensitive to pH, heat, metal ions, and light, further complicating its conjugation chemistry [78]. One conjugation strategy is to couple the terminal carboxylate of PLA with Doxo by creating an amide linkage through the 3'-NH<sub>2</sub> of Doxo [39,79]. Such Doxo-PLA conjugates, however, cannot release Doxo in its original form by hydrolysis.

Instead, Doxo-3'-lactamide, a prodrug of Doxo, is formed, which does not easily degrade *in vivo* due to the stability of amide bond [80]. Other efforts have been devoted to conjugation between the C13-ketone group of Doxo and hydrazine groups of polymeric carriers by forming an acid-labile hydrazone bond [22,81–83]. However, clinical studies of immunoconjugates with Doxo connected to monoclonal antibodies via hydrazone linkers gave unsatisfactory antitumor effects, ultimately leading to the termination of the clinical development of such immunoconjugates [84].

In previous studies involving the use of metal catalysts for LA polymerization, ROP of LA proceeded predominately by metal-alkoxides (M-ORs) rather than by metal-amides (M-NHRs) [47]. M-OR complexes typically have higher activities for LA ring opening than their amine analogs. For instance, Coates and coworkers reported that (BDI)ZnOCH(CH<sub>3</sub>)<sub>2</sub> initiated and completed an LA polymerization within 20 min at a M/I ratio of 200 while a similar polymerization mediated by (BDI)ZnN(TMS)<sub>2</sub> required 10 h to complete [41]. The chemoselectivity of -OH instead of -NH<sub>2</sub> for Zn catalysts has also been confirmed by another molecular pair, 1-pyrenemethanol (Pyr-OH) and 1-pyrenemethylamine (Pyr-NH<sub>2</sub>) [52].

Doxo has three hydroxyl groups, one at each of its C4', C9, and C14 positions. Theoretically, LA polymerization can be initiated by any or all of these hydroxyl groups. C9-OH is the most sterically hindered and thus unlikely to initiate polymerization. To evaluate the initiation regioselectivity, we mixed Doxo with the catalyst (BDI-II)ZnN(TMS)<sub>2</sub> and succinic anhydride (SA) to mimic the initiation step of LA polymerization. ESI-MS results coupled with NMR analysis revealed that the SA ring was opened by the C14-OH of Doxo rather than by the C4'-OH or C3'-NH<sub>2</sub> of Doxo. When (BDI-II)ZnN(TMS)<sub>2</sub> was replaced by Zn(N(TMS)<sub>2</sub>)<sub>2</sub>, a Zn catalyst without ligands, the initiation regioselectivity completely disappeared, with Doxo-4', 14-bissuccinic ester (Doxo-2SA), and Doxo-4', 9, 14-trisuccinic ester (Doxo-3SA) being the predominant products (Figure 7.6). Interestingly, the metal activity also had a profound effect on regioselectivity. When the more highly active (BDI-II)MgN(TMS)<sub>2</sub> catalyst was used in a similar reaction, the most prevalent product was Doxo-2SA. Thus, by rationally designing ROP metal catalysts, Doxo-PLA conjugates with highly controlled regio- and chemoselectivity are achievable within one step without having to protect the C3'-NH<sub>2</sub> and other competing hydroxyl groups of Doxo [52].

Having completed preliminary investigations with SA, we next studied Doxo-initiated LA polymerization. Doxo/(BDI-II)ZnN(TMS)<sub>2</sub>-mediated LA polymerization resulted in Doxo-PLA with narrow MWD (<1.2) and the expected MWs. At a low M/I ratio of 10, the drug loading was as high as 27.4% (Doxo-LA<sub>10</sub>). To our knowledge, this is by far the highest loading ever reported in Doxo-containing polymeric NPs [52]. HPLC analysis revealed that Doxo-LA<sub>10</sub> conjugates incubated in PBS at 30°C released Doxo in its original, therapeutically active form. In a separate experiment, Doxo-LA<sub>100</sub> treated with 0.1 M NaOH was shown to release 88–92% of the Doxo in its original form. In this case, the incomplete recovery is likely due to instability of Doxo in NaOH. Combined, these studies suggest that Doxo molecules were linked to PLA through its hydroxyl group(s) by forming ester linker(s) with PLA, which could be hydrolyzed in an alkaline condition. Even at high



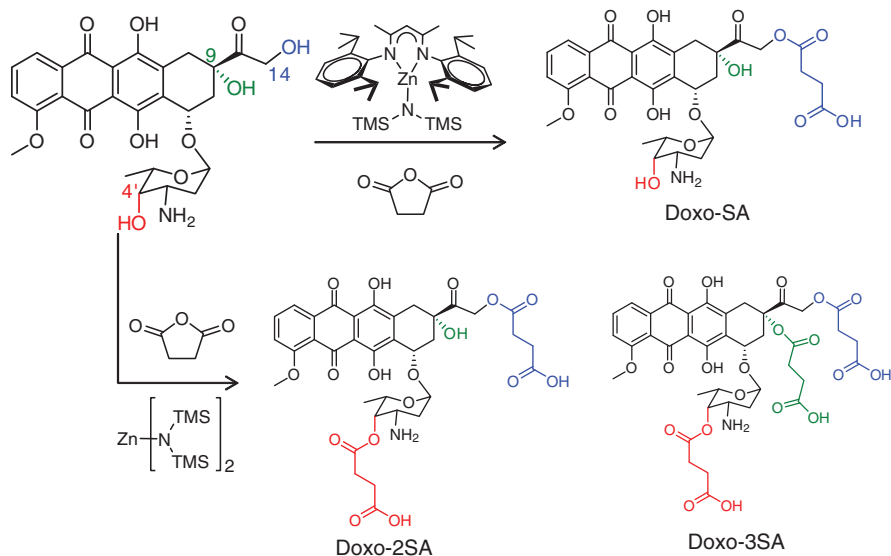


**FIGURE 7.6** Scheme of Doxo-SA reaction (1:3 molar ratio) mediated by different Zn catalysts.

drug loading (27.4%), sustained release of Doxo from Doxo-LA<sub>10</sub> NC was observed without burst release. This is in sharp contrast to the burst release of PLA/Doxo NPs prepared by co-precipitation, in which 90% of the Doxo is released within 3 h [52]. The sustained release of Doxo from NCs with high loading may help alleviate the systemic side effects of Doxil<sup>TM</sup> without reducing the overall dosage.

## 7.4 NANOCONJUGATES: FORMULATION AND POTENTIAL APPLICATION

### 7.4.1 Formulation

Particle size is an important aspect of drug delivery. For cancer therapeutics, formulated particles should have a uniform, monomodal distribution and a diameter <200 nm to take advantage of the enhanced permeability and retention (EPR) effect. As such, particles formed by nanoprecipitation of Ptx1-PLA were evaluated for their size. In general, Ptx1-PLA yielded particles with monomodal distributions while their nanoencapsulate (NEs, see Section 7.2.1) counterparts were polydisperse (Figure 7.7a) [13,85]. As the multimodal distribution of NEs is due in part to the aggregation of nonencapsulated free drug [13], the monomodal distribution observed with NCs is likely related to the unimolecular structure of Ptx1-PLA conjugates. The actual size of Ptx1-PLA NPs prepared by nanoprecipitation can be manipulated by changing the solvent as well as polymer concentration. At a fixed Ptx1-PLA concentration, the size of NCs prepared by precipitating a DMF solution of conjugate

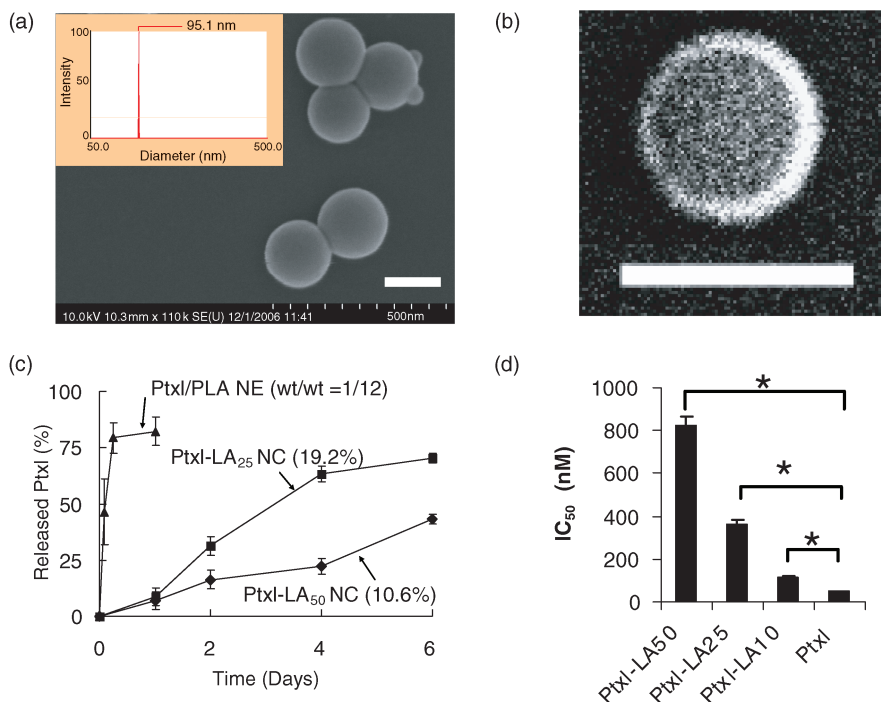


**FIGURE 7.7** (a) Ptxl-LA<sub>25</sub> NCs were analyzed by dynamic light scattering (DLS) and scanning electron microscopy (SEM). (b) SEM image of Ptxl-LA<sub>25</sub>/PLGA-mPEG NCs (Scale bar = 150 nm). The different density of materials were indicated with different gray scale: PEG layer (white color) and hydrophobic PLA part (gray color) (c) Release kinetics of Ptxl from Ptxl-PLA NCs and Ptxl-PLA NE (Prepared by nanoprecipitation of a mixture of Ptxl and PLA (Ptxl-PLA (wt/wt) = 1/12) at 37°C in PBS). (d) IC<sub>50</sub> values determined by MTT assay of Ptxl-PLA NCs and free Ptxl, which were incubated with PC-3 cells for 24 h. (Source: Figures reproduced with permission from Reference [51].)

is typically in a range 60–100 nm, 20–30 nm smaller than those prepared with acetone or THF as a solvent [13]. When nanoprecipitation is carried out using a 1:20 (v:v) mixture of DMF and water, the size of Ptxl-LA NCs shows a linear correlation with the conjugate concentration and can be used to precisely form particles with diameters from 60 to 100 nm.

Surface modification of NPs with PEG is widely used for prolonged systemic circulation and reduced aggregation of NPs in blood [86]. To avoid the removal of unreacted reagents and by-products, poly(lactide)-*b*-methoxylated PEG (PLA-mPEG)—an amphiphilic copolymer that has a 14 kDa PLA and a 5 kDa PEG segment [87]—was used to PEGylate NCs instead of covalently conjugating PEG to NCs [65,85]. The PEGylated structure of the NCs can be seen by scanning transmission electron microscopy (Figure 7.7b). Ptxl-LA NCs with a PEGylated surface have a negative surface zeta potential and thus remain nonaggregated in water and PBS solution by means of surface charge repulsion. In addition, we also

developed a one-step co-precipitation method to formulate NCs that could stay nonaggregated in a salt solution with an amphiphilic triblock copolymer PLA-PEG-PLA, a feature that diblock PLA-PEG did not provide [55].

Drug burst release is a long-standing formulation challenge to NEs and often results in undesirable side effects and reduced therapeutic efficacy [67]. Conventional NEs typically show burst release of 60–90% of their payload within a few to tens of hours [9]. Since the Ptxl release kinetics of Ptxl-PLA NCs is determined not simply by diffusion—as is the case with NEs—but by the hydrolysis of the Ptxl-PLA ester linker followed by diffusion out of NCs, the release kinetics of Ptxl from NCs are more controlled and show significantly reduced burst release (Figure 7.7c). For example, Ptxl released from Ptxl-LA<sub>25</sub> NCs (19.2 wt%) was 8.7% at Day 1 and 70.4% at Day 6. In comparison, 89% of Ptxl was released within 24 h from Ptxl/PLA NE (Figure 7.7c). Release of Ptxl from Ptxl-LA<sub>50</sub> NCs was slower than from Ptxl-LA<sub>25</sub> NCs, presumably because of the higher MW of Ptxl-LA<sub>50</sub> and more compact particle structure. With its controlled drug release, the *in vitro* toxicity of Ptxl-LA NCs correlates with the amount of Ptxl released (Figure 7.7d). For example, Ptxl-LA<sub>15</sub> NCs have a nearly identical IC<sub>50</sub> to free Ptxl (87 nM) while the IC<sub>50</sub> of Ptxl-LA<sub>50</sub> NCs is an order of magnitude higher. As a result, the toxicity of NCs can be tuned in a wide range simply by controlling NC drug loading.

Aptamers are either single-stranded DNA or RNA that specifically binds to target ligands [88,89]. When used for cancer targeting, aptamers are capable of binding to target antigens with extremely high affinity and specificity in a manner resembling antibody-mediated cancer targeting [90,91]. Unlike antibodies, synthesis of aptamers is an entirely chemical process and thus shows negligible batch-to-batch inconsistency [92,93]. Moreover, aptamers are typically nonimmunogenic and exhibit remarkable stability against pH, temperature, and solvent. The A10 aptamer with 2'-fluoro-modified ribose on all pyrimidines and a 3'-inverted deoxythymidine cap has been identified and utilized to target extracellular prostate-specific membrane antigen (PSMA) [94]. A10 binds to PSMA-positive LNCaP prostate cancer cells but not PSMA-negative PC-3 prostate cancer cells. To demonstrate NC targeting, amine-terminated A10 aptamer was conjugated to PLA-PEG-COOH/Cy5-PLA NCs through carboxylic acid-amine coupling in the presence of EDC and NHS to give aptamer/PLA-PEG-COOH/Cy5-PLA NCs (aptamer-Cy5 NC) [90]. Incubation of aptamer-Cy5 NCs with LNCaP cells for 6 h resulted in substantially increased NC internalization (Figure 7.8) compared to PC-3 cells. These *in vitro* studies demonstrated that NCs conjugated with aptamer-targeting ligand can potentially be used for prostate cancer targeting.

Small-scale NPs that stay nonaggregated in PBS for *in vitro* or *in vivo* laboratory studies are straightforward. However, in order to facilitate clinical translation, NPs need to be prepared in large quantity with well-controlled properties that remain unchanged during the processes of manufacturing, storage, and transport. Because Ptxl is covalently conjugated to PLA through an ester bond that is subject to hydrolysis upon exposure to water, handling of Ptxl-PLA NCs in aqueous solution is undesirable. Thus, NCs have to be formulated in solid form for clinical use. By screening various molecules, we discovered that albumin functions as an excellent

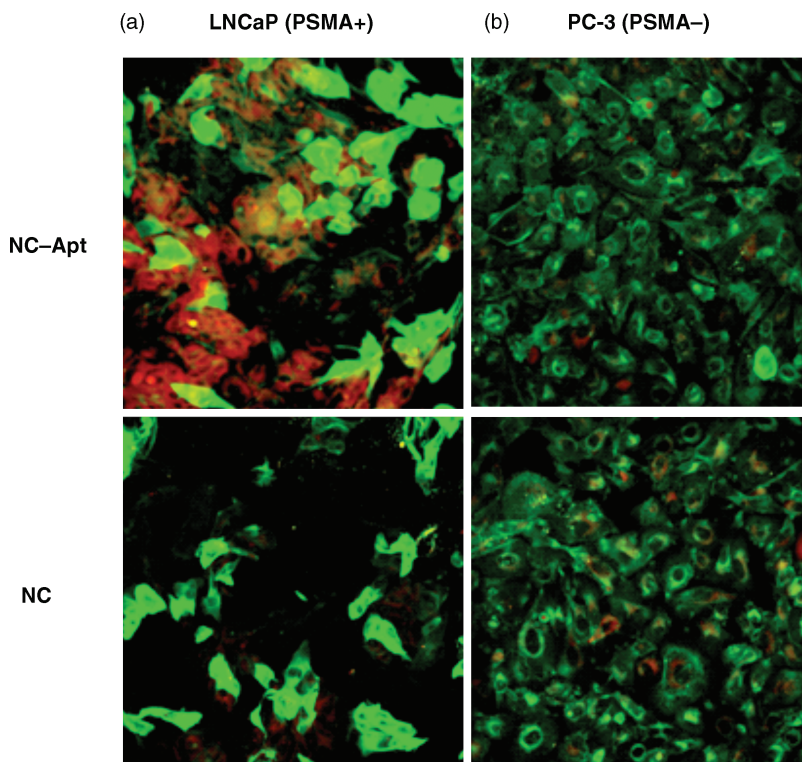


**FIGURE 7.8** Confocal images of LNCaP (a) and PC-3 (b) cells treated with aptamer-functionalized nanoconjugates (NC-Apt, top) and nanoparticles without aptamer (NC, bottom). The Cy-5 incorporated NC or NC-Apt are shown in red. The cells counter stained with Alexa-Fluor 488 Phalloidin (binding to cellular actin) are shown in green.

lyoprotectant for PtxI-PLA and yields solid NCs that do not aggregate when reconstituted in PBS. By incorporating the albumin-based lyoprotection technique, we demonstrated for the first time that polymer nanoparticles containing a conjugated nucleic acid targeting ligand can be prepared in solid form and still be reconstituted to well-dispersed, nonaggregated particles with functional targeting capability [55].

#### 7.4.2 Theranostic Nanoconjugates

There is growing interest in developing noninvasive, whole-body fluorescent imaging techniques to assess the biodistribution of drug delivery systems or diagnostic agents within patients. To ensure effective measurement of fluorescent signal *in vivo*, it is crucial to use red or near-IR dyes. Quantum dots, a class of inorganic nanocrystals with excellent fluorescent intensity and photostability, can readily be prepared to have a far-red emission band. However, there is a general consensus

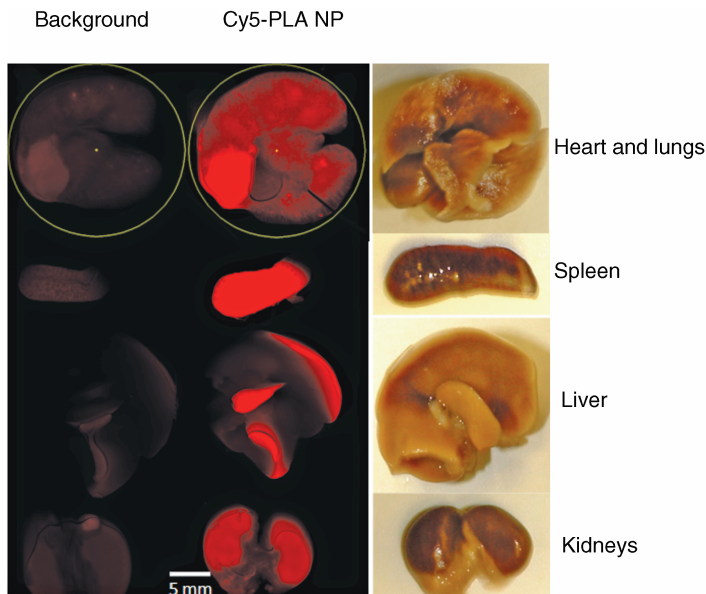


**FIGURE 7.9** Distribution of Cy5 dye-labeled PLA NCs in various visceral mice organs. Mice were sacrificed 24 h after i.v. injection of Cy5-PLA NCs.

that quantum dots cannot be used in humans because of their toxicity. Currently, small molecule organic dyes are more promising probes to be coupled with imaging systems for clinical applications as compared to quantum dots. Polymeric nanoparticles can function as good carriers for the delivery of small molecule imaging materials because they can provide prolonged systemic circulation and improved tumor accumulation compared to unformulated drugs. To meet this challenge, it is particularly important that NPs be formulated with stably incorporated fluorescent ligands and controlled formulation parameters (size, surface properties, etc.). Accordingly, our monomodal, narrowly distributed PEGylated Cy5-PLA NPs have the potential to be candidates for whole body *in vivo* imaging. Preliminary *in vivo* studies demonstrated that Cy5-PLA NCs can be easily visualized in various visceral organs with low autofluorescent background ratios (Figure 7.9). Owing to their sub-100 nm size, the Cy5-PLA NCs also can be used to study the lymphatic biodistribution of NPs when coupled with whole-body optical imaging [95]. These promising results support the further development of Cy5-PLA NCs as a model system to assess the *in vivo* pharmacological and pharmacokinetics profiles of NCs.

### 7.4.3 Nanoconjugates Against Other Diseases

Considering that molecular targeting of cell-based targets may be confounded by inter- or intra-patient heterogeneity in cell surface antigen expression, targeted NPs that can recognize the extracellular matrix have attracted considerable attention for

therapeutic/diagnostic delivery. We have recently engineered a peptide-conjugated NP to target the vascular basement membrane for the treatment of injured vasculature. The high affinity C11 peptide was screened from a combinatorial phage library of hepta-peptide ligands against human collagen IV, which represents 50% of the vascular basement membrane (Figure 7.10) [96]. Angioplasty-injured carotid artery

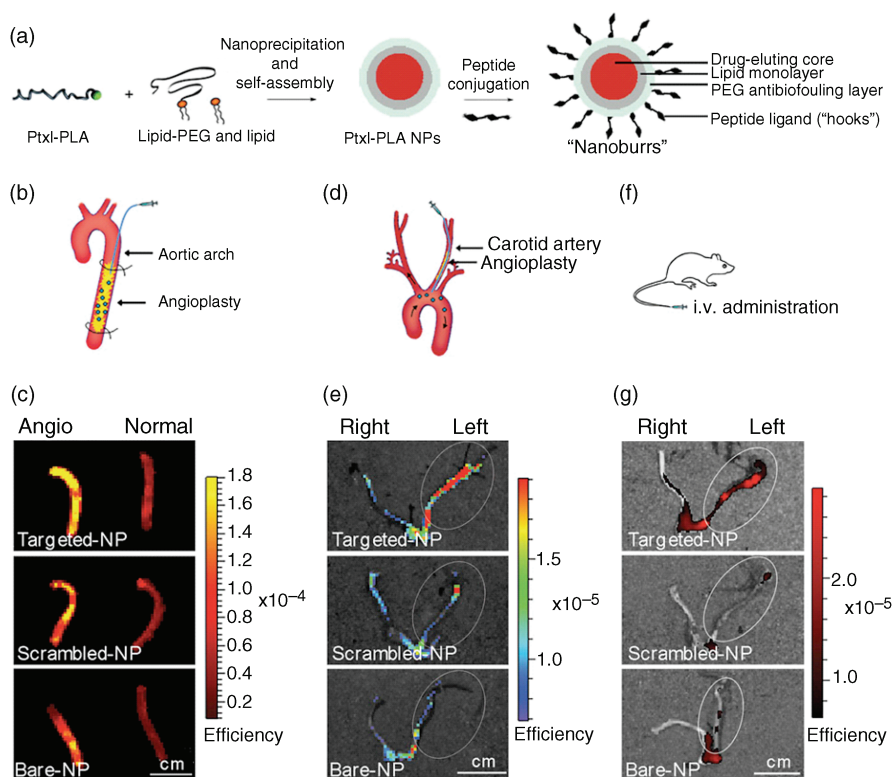


**FIGURE 7.10** (a) Schematic of NPs synthesis by nanoprecipitation and self-assembly of Ptxl-PLA NCs with lipids and peptide ligands to adhere to the exposed basement membrane during vascular injury. (b) Scheme of *ex vivo* abdominal aorta injury model; samples were delivered into the aorta segment for 5 min. (c) Fluorescence images overlaid on photographs of balloon-injured aortas incubated with NCs with a targeting peptide, compared with scrambled-peptide and nontargeted NPs. (d) *In vivo* intra-aortic administration in a carotid injury model: a catheter was inserted via the external carotid into the common carotid and advanced into the aortic arch. (e) Fluorescence images overlaid on photographs of carotid arteries incubated with NCs with a targeting peptide, compared with scrambled-peptide and nontargeted NPs. (f) *In vivo* systemic administration in a carotid angioplasty model. (g) Fluorescence images overlaid on photographs of carotid arteries incubated with NCs with a targeting peptide, compared with scrambled-peptide and nontargeted NPs. For imaging, Alexa Fluor 647-PLGA dye conjugates were encapsulated in place of Ptxl-PLA drug conjugates. (Scale bar, 1 cm.)

was used as a model of compromised vasculature to examine the targeting capacity of the C11 peptide-conjugated polymeric NPs. The targeted NPs were delivered via both intra-arterial and i.v. administration and, when compared to nontargeted NPs, showed greater *in vivo* vascular retention at sites of injured vasculature in rats (Figure 7.10) [96]. Although the initial application was for vessel wall targeting in cardiovascular disease, the utility of this peptide-targeted NP system is broad and could be used to diagnose and treat different human diseases where the endothelial lining is compromised.

Immunosuppressive agents have played a pivotal role in ensuring the success of organ transplantation and greatly improved the outcomes of patients with life-threatening, immune-mediated diseases [97]. However, the use of immunosuppressive agents is hindered by the lack of selectivity as well as major adverse drug reactions. The immunosuppressive agent cyclosporine (CsA), for example, results in a dramatic improvement in short-term allograft survival but also poses a risk of chronic nephrotoxicity because of its narrow therapeutic window [98–100]. We recently developed CsA–PLA NCs to achieve targeted immunosuppression for a wide variety of immune-mediated disorders [101]. CsA–PLA NCs showed superior physicochemical properties with excellent size control, narrow size distribution, and very well controlled release kinetics without a noticeable burst release. CsA–PLA NCs also showed excellent stability in biological media with negligible aggregation. Because of their ability to mediate the sustained release of CsA *in vitro* while suppressing T-cell mediated immune responses, CsA–PLA NCs are an excellent system for immunosuppression of organ rejection. We also developed a novel strategy combining CsA–PLA NCs with dendritic cells (DCs) to efficiently deliver CsA to draining lymph nodes to inhibit T-cell priming in a locally controlled and sustained manner without systemic release. This innovative delivery strategy constitutes a strong basis for future targeted delivery of immunosuppressive drugs with improved efficiency and reduced toxicity.

## 7.5 CONCLUSIONS AND OUTLOOK

LA ROP-mediated drug conjugation allows for facile regio- and chemoselective incorporation of drugs onto PLA. This in turn allows for the formation of drug delivery vehicles with low polydispersity, predetermined drug loadings (up to ~30%), and quantitative loading efficiencies. The BDI–metal chelating complexes described earlier for Cpt, Ptxl, and Doxo conjugation do not have deleterious effects on drugs and can be easily removed by solvent extraction. Because both Zn and Mg ions are biocompatible and, in fact, are key elements in our dietary mineral supplements, there should be no significant safety concerns regarding the use of these two metal catalysts. Multigram scales of drug-PLA conjugates can be readily prepared within hours using the one-pot polymerization approaches described here. Because drug molecules are covalently conjugated to PLA, the post-reaction formulation process (precipitation, removal of catalysts, nanoprecipitation, sterilization, lyophilization, shipping and handling, etc.) has minimal impact on sample

property as compared to drug-polymer NPs prepared via encapsulation methods. This polymerization-mediated conjugation method may be utilized for the formulation of polymer-drug conjugates not only for drug delivery, but also for other controlled release applications (scaffolds, coatings of stents, etc.). Other cyclic esters (e.g.,  $\epsilon$ -caprolactone and  $\delta$ -valerolactone) are likely to replace LA and find use as monomers in such drug-initiated polymerizations [102]. The drug/(BDI-X)  $\text{ZnN}(\text{TMS})_2$ -initiated polymerization of these cyclic esters at room temperature has recently been achieved in our laboratory, which will provide further tunability of the release profiles and other physicochemical properties. Given that the lack of a controlled formulation for nanoparticulate drug delivery vehicles is one of the bottlenecks to their clinical development, this unique, ROP-mediated conjugation methodology may contribute to the development of clinically applicable nanomedicines.

Although there has been impressive progress in nanomedicine for cancer treatment in the past few years, enormous tasks remain. The convergence of seemingly disparate scientific fields (e.g., cancer biology, electronics, bioimaging, biomicroelectromechanical systems, computer science, polymer and materials chemistry, biophysics) will only accelerate the development of nanomedicine [103]. Our work will continue in the daunting task of pushing targeted nanoconjugates for clinical evaluation, with the expansion of our technology to other disease-related formulations (e.g., imaging agents or implantable devices). It also will be important to improve intratumoral penetration for enhanced efficacy [104,105]. Given the limitations of spatial and temporal changes in the expression of the target [106], the seemingly pedestrian issues on targeting ligand functionality are also likely to be challenging *in vivo* [107,108]. The prevention and treatment of metastasis will be of particular interest because metastasis is responsible for 90% of cancer deaths [109]. The coordination of different approaches will help optimize the delivery efficiency. A deep understanding of all aspects of the biology of cancers, including tumor microenvironment, will continue to be crucial for design and understanding [110]. We are far from being able to create delivery vehicles to meet the expectation of complete tumor eradication. However, as the field of nanomedicine matures, the objective may be on the horizon.

## Acknowledgments

Jianjun Cheng acknowledges support from the NSF (Career Award Program DMR-0748834) and the NIH (NIH Director's New Innovator Award 1DP2OD007246-01, 1R21EB009486A, and 1R21CA139329Z). Rong Tong acknowledges a student fellowship from the Siteman Center for Cancer Nanotechnology Excellence (University of Washington & University of Illinois at Urbana-Champaign) from 2007 to 2010. Li Tang was funded at University of Illinois at Urbana-Champaign from NIH National Cancer Institute Alliance for Nanotechnology in Cancer "Midwest Cancer Nanotechnology Training Center" Grant R25 CA154015A.



## REFERENCES

1. Langer, R. (1998). Drug delivery and targeting. *Nature* 392, 5.
2. Davis, M. E., Chen, Z., Shin, D. M. (2008). Nanoparticle therapeutics: an emerging treatment modality for cancer. *Nature Reviews Drug Discovery* 7, 771.
3. Petros, R. A., DeSimone, J. M. (2010). Strategies in the design of nanoparticles for therapeutic applications. *Nature Reviews Drug Discovery* 9, 615.
4. Wagner, V., Dullaart, A., Bock, A. K., Zweck, A. (2006). The emerging nanomedicine landscape. *Nature Biotechnology* 24, 1211.
5. Zhang, L., Gu, F. X., Chan, J. M., Wang, A. Z., Langer, R. S., Farokhzad, O. C. (2008). Nanoparticles in medicine: therapeutic applications and developments. *Clinical Pharmacology and Therapeutics* 83, 761.
6. Farokhzad, O. C., Langer, R. (2009). Impact of nanotechnology on drug delivery. *ACS Nano* 3, 16.
7. Cohen, S., Yoshioka, T., Lucarelli, M., Hwang, L. H., Langer, R. (1991). Controlled delivery systems for proteins based on poly(lactic glycolic acid) microspheres. *Pharmaceutical Research* 8, 713.
8. Ringsdorf, H. (1975). Structure and properties of pharmacologically active polymers. *Journal of Polymer Science Part C-Polymer Symposium* 51, 135.
9. Musumeci, T., Ventura, C. A., Giannone, I., Ruozi, B., Montenegro, L., Pignatello, R., Puglisi, G. (2006). PLA/PLGA nanoparticles for sustained release of docetaxel. *International Journal of Pharmaceutics* 325, 172.
10. Tong, R., Cheng, J. J. (2007). Anticancer polymeric nanomedicines. *Polymer Reviews (Philadelphia, PA, US)* 47, 345.
11. Hamblett, K. J., Senter, P. D., Chace, D. F., Sun, M. M. C., Lenox, J., Cervený, C. G., Kissler, K. M., Bernhardt, S. X., Kopcha, A. K., Zabinski, R. F., Meyer, D. L., Francisco, J. A. (2004). Effects of drug loading on the antitumor activity of a monoclonal antibody drug conjugate. *Clinical Cancer Research* 10, 7063.
12. Schluep, T., Hwang, J., Cheng, J. J., Heidel, J. D., Bartlett, D. W., Hollister, B., Davis, M. E. (2006). Preclinical efficacy of the camptothecin-polymer conjugate IT-101 in multiple cancer models. *Clinical Cancer Research* 12, 1606.
13. Cheng, J., Teplý, B. A., Sherifi, I., Sung, J., Luther, G., Gu, F. X., Levy-Nissenbaum, E., Radovic-Moreno, A. F., Langer, R., Farokhzad, O. C. (2007). Formulation of functionalized PLGA-PEG nanoparticles for *in vivo* targeted drug delivery. *Biomaterials* 28, 869.
14. Duncan, R. (2006). Polymer conjugates as anticancer nanomedicines. *Nature Reviews Cancer* 6, 688.
15. Duncan, R. (2003). The dawning era of polymer therapeutics. *Nature Reviews Drug Discovery* 2, 347.
16. Cheng, J., Khin, K. T., Jensen, G. S., Liu, A. J., Davis, M. E. (2003). Synthesis of linear, beta-cyclodextrin-based polymers and their camptothecin conjugates. *Bioconjugate Chemistry* 14, 1007.
17. Schluep, T., Hwang, J., Hildebrandt, I. J., Czernin, J., Choi, C. H. J., Alabi, C. A., Mack, B. C., Davis, M. E. (2009). Pharmacokinetics and tumor dynamics of the nanoparticle IT-101 from PET imaging and tumor histological measurements. *Proceedings of the National Academy of Sciences of the United States of America* 106, 11394.

18. Davis, M. E. (2009). Design and development of IT-101, a cyclodextrin-containing polymer conjugate of camptothecin. *Advanced Drug Delivery Reviews* 61, 1189.
19. Davis, M. E., Zuckerman, J. E., Choi, C. H. J., Seligson, D., Tolcher, A., Alabi, C. A., Yen, Y., Heidel, J. D., Ribas, A. (2010). Evidence of RNAi in humans from systemically administered siRNA via targeted nanoparticles. *Nature* 464, 1067.
20. Davis, M. E. (2009). The first targeted delivery of siRNA in humans via a self-assembling, cyclodextrin polymer-based nanoparticle: from concept to clinic. *Molecular Pharmaceutics* 6, 659.
21. Fox, M. E., Szoka, F. C., Frechet, J. M. J. (2009). Soluble polymer carriers for the treatment of cancer: the importance of molecular architecture. *Accounts of Chemical Research* 42, 1141.
22. Lee, C. C., Gillies, E. R., Fox, M. E., Guillaudeu, S. J., Frechet, J. M. J., Dy, E. E., Szoka, F. C. (2006). A single dose of doxorubicin-functionalized bow-tie dendrimer cures mice bearing C-26 colon carcinomas. *Proceedings of the National Academy of Sciences of the United States of America* 103, 16649.
23. [http://en.wikipedia.org/wiki/List\\_of\\_bestselling\\_drugs](http://en.wikipedia.org/wiki/List_of_bestselling_drugs).
24. Lee, C. C., MacKay, J. A., Frechet, J. M. J., Szoka, F. C. (2005). Designing dendrimers for biological applications. *Nature Biotechnology* 23, 1517.
25. Srinivasachari, S., Fichter, K. M., Reineke, T. M. (2008). Polycationic beta-cyclodextrin "Click Clusters": monodisperse and versatile scaffolds for nucleic acid delivery. *Journal of the American Chemical Society* 130, 4618.
26. Lu, H., Cheng, J. (2008). Controlled ring-opening polymerization of alpha-amino acid *N*-carboxyanhydrides and facile end group functionalization of polypeptides. *Journal of the American Chemical Society* 130, 12562.
27. Lu, H., Cheng, J. (2007). Hexamethyldisilazane-mediated controlled polymerization of alpha-amino acid *N*-carboxyanhydrides. *Journal of the American Chemical Society* 129, 14114.
28. Cheng, J., Deming, T. J. (2001). Controlled polymerization of beta-lactams using metal-amido complexes: synthesis of block copoly(beta-peptides). *Journal of the American Chemical Society* 123, 9457.
29. Medina, S. H., El-Sayed, M. E. H. (2009). Dendrimers as carriers for delivery of chemotherapeutic agents. *Chemical Reviews* 109, 3141.
30. Gillies, E. R., Frechet, J. M. J. (2002). Designing macromolecules for therapeutic applications: polyester dendrimer-poly(ethylene oxide) "bow-tie" hybrids with tunable molecular weight and architecture. *Journal of the American Chemical Society* 124, 14137.
31. Liu, G., Jia, L. (2004). Design of catalytic carbonylative polymerizations of heterocycles. Synthesis of polyesters and amphiphilic poly(amide-block-ester)s. *Journal of the American Chemical Society* 126, 14716.
32. Zhang, X. F., Li, Y. X., Chen, X. S., Wang, X. H., Xu, X. Y., Liang, Q. Z., Hu, J. L., Jing, X. B. (2005). Synthesis and characterization of the paclitaxel/MPEG-PLA block copolymer conjugate. *Biomaterials* 26, 2121.
33. Cheng, J., Khin, K. T., Davis, M. E. (2004). Antitumor activity of beta-cyclodextrin polymer-camptothecin conjugates. *Molecular Pharmaceutics* 1, 183.
34. Shen, Y. Q., Jin, E. L., Zhang, B., Murphy, C. J., Sui, M. H., Zhao, J., Wang, J. Q., Tang, J. B., Fan, M. H., Van Kirk, E., Murdoch, W. J. (2010). Prodrugs forming high drug loading

- multifunctional nanocapsules for intracellular cancer drug delivery. *Proceedings of the National Academy of Sciences of the United States of America* 132, 4259.
35. Kim, S. C., Kim, D. W., Shim, Y. H., Bang, J. S., Oh, H. S., Kim, S. W., Seo, M. H. (2001). *In vivo* evaluation of polymeric micellar paclitaxel formulation: toxicity and efficacy. *Journal of Controlled Release* 72, 191.
  36. Benny, O., Fainaru, O., Adini, A., Cassiola, F., Bazinet, L., Adini, I., Pravda, E., Nahmias, Y., Koirala, S., Corfas, G., D'Amato, R. J., Folkman, J. (2008). An orally delivered small-molecule formulation with antiangiogenic and anticancer activity. *Nature Biotechnology* 26, 799.
  37. Lee, S. H., Zhang, Z. P., Feng, S. S. (2007). Nanoparticles of poly(lactide): tocopheryl polyethylene glycol succinate (PLA-TPGS) copolymers for protein drug delivery. *Biomaterials* 28, 2041.
  38. Zhang, Z. P., Feng, S. S. (2006). Nanoparticles of poly(lactide)/vitamin E TPGS copolymer for cancer chemotherapy: synthesis, formulation, characterization and *in vitro* drug release. *Biomaterials* 27, 262.
  39. Sengupta, S., Eavarone, D., Capila, I., Zhao, G. L., Watson, N., Kiziltepe, T., Sasisekharan, R. (2005). Temporal targeting of tumour cells and neovasculature with a nanoscale delivery system. *Nature* 436, 568.
  40. Yoo, H. S., Lee, K. H., Oh, J. E., Park, T. G. (2000). *In vitro* and *in vivo* anti-tumor activities of nanoparticles based on doxorubicin-PLGA conjugates. *Journal of Controlled Release* 68, 419.
  41. Chamberlain, B. M., Cheng, M., Moore, D. R., Ovitt, T. M., Lobkovsky, E. B., Coates, G. W. (2001). Polymerization of lactide with zinc and magnesium beta-diiminate complexes: stereocontrol and mechanism. *Journal of the American Chemical Society* 123, 3229.
  42. O'Keefe, B. J., Hillmyer, M. A., Tolman, W. B. (2001). Polymerization of lactide and related cyclic esters by discrete metal complexes. *Journal of the Chemical Society-Dalton Transactions* 2215.
  43. Cheng, J., Deming, T. J. (2001). Synthesis and conformational analysis of optically active poly(beta-peptides). *Macromolecules* 34, 5169.
  44. Lu, H., Cheng, J. (2008). *N*-trimethylsilyl amines for controlled ring-opening polymerization of amino acid *N*-carboxyanhydrides and facile end group functionalization of polypeptides. *Journal of the American Chemical Society* 130, 12562.
  45. Ouchi, M., Terashima, T., Sawamoto, M. (2009). Transition metal-catalyzed living radical polymerization: toward perfection in catalysis and precision polymer synthesis. *Chemical Reviews* 109, 4963.
  46. Dechy-Cabaret, O., Martin-Vaca, B., Bourissou, D. (2004). Controlled ring-opening polymerization of lactide and glycolide. *Chemical Reviews* 104, 6147.
  47. du Boullay, O. T., Marchal, E., Martin-Vaca, B., Cossio, F. P., Bourissou, D. (2006). An activated equivalent of lactide toward organocatalytic ring-opening polymerization. *Journal of the American Chemical Society* 128, 16442.
  48. Hu, Y., Jiang, X., Ding, Y., Zhang, L., Yang, C., Zhang, J., Chen, J., Yang, Y. (2003). Preparation and drug release behaviors of nimodipine-loaded poly(caprolactone)-poly(ethylene oxide)-poly(lactide) amphiphilic copolymer nanoparticles. *Biomaterials* 24, 2395.

49. Chen, F., Gao, Q., Hong, G., Ni, J. (2008). Synthesis of magnetite core-shell nanoparticles by surface-initiated ring-opening polymerization of L-lactide. *Journal of Magnetism and Magnetic Materials* 320, 1921.
50. Cheng, M., Attygalle, A. B., Lobkovsky, E. B., Coates, G. W. (1999). Single-site catalysts for ring-opening polymerization: synthesis of heterotactic poly(lactic acid) from rac-lactide. *Journal of the American Chemical Society* 121, 11583.
51. Tong, R., Cheng, J. (2008). Paclitaxel-initiated, controlled polymerization of lactide for the formulation of polymeric nanoparticulate delivery vehicles. *Angewandte Chemie (International edition)* 47, 4830.
52. Tong, R., Cheng, J. (2009). Ring-opening polymerization-mediated controlled formulation of polylactide-drug nanoparticles. *Journal of the American Chemical Society* 131, 4744.
53. Moore, D. R., Cheng, M., Lobkovsky, E. B., Coates, G. W. (2002). Electronic and steric effects on catalysts for CO<sub>2</sub>/epoxide polymerization: subtle modifications resulting in superior activities. *Angewandte Chemie (International edition)* 41, 2599.
54. Tong, R., Cheng, J. (2010). Controlled synthesis of camptothecin-poly(lactide) conjugates and nanoconjugates. *Bioconjugate Chemistry* 21, 111.
55. Tong, R., Yala, L., Fan, T. M., Cheng, J. (2010). The formulation of aptamer-coated paclitaxel-poly(lactide) nanoconjugates and their targeting to cancer cells. *Biomaterials* 31, 3043.
56. Hertzberg, R. P., Caranfa, M. J., Hecht, S. M. (1989). On the mechanism of topoisomerase-I inhibition by camptothecin: evidence for binding to an enzyme DNA complex. *Biochemistry* 28, 4629.
57. Muggia, F. M., Dimery, I., Arbuck, S. G., *Camptothecin and its analogs: an overview of their potential in cancer therapeutics*, Academy of Sciences, New York, 1996.
58. Mi, Z. H., Burke, T. G. (1994). Differential interactions of camptothecin lactone and carboxylate forms with human blood components. *Biochemistry* 33, 10325.
59. Mi, Z. H., Burke, T. G. (1994). Marked interspecies variations concerning the interactions of camptothecin with serum albumins: a frequency-domain fluorescence spectroscopic study. *Biochemistry* 33, 12540.
60. Cheng, J., Khin, K. T., Davis, M. E. (2004). Antitumor activity of beta-cyclodextrin polymer: camptothecin conjugates. *Molecular Pharmaceutics* 1, 183.
61. Kunii, R., Onishi, H., Machida, Y. (2007). Preparation and antitumor characteristics of PLA(PEG-PPG-PEG) nanoparticles loaded with camptothecin. *European Journal of Pharmaceutics and Biopharmaceutics* 67, 9.
62. Li, C. (1998). Complete regression of well-established tumors using a novel water-soluble poly(L-glutamic acid)-paclitaxel conjugate. *Cancer Research* 58, 2404.
63. Singer, J. W. (2005). Paclitaxel poliglumex (XYOTAX, CT-2103): a macromolecular taxane. *Journal of Controlled Release* 109, 120.
64. Fonseca, C., Simoes, S., Gaspar, R. (2002). Paclitaxel-loaded PLGA nanoparticles: preparation, physicochemical characterization and *in vitro* anti-tumoral activity. *Journal of Controlled Release* 83, 273.
65. Gref, R., Minamitake, Y., Peracchia, M., Trubetskoy, V. S., Torchilin, V. P., Langer, R. (1994). Biodegradable long-circulating polymeric nanospheres. *Science* 263, 1600.
66. Panyam, J., Labhasetwar, V. (2003). Biodegradable nanoparticles for drug and gene delivery to cells and tissue. *Advanced Drug Delivery Reviews* 55, 329.

67. Soppimath, K. S., Aminabhavi, T. M., Kulkarni, A. R., Rudzinski, W. E. (2001). Biodegradable polymeric nanoparticles as drug delivery devices. *Journal of Controlled Release* 70, 1.
68. Mastropaolo, D., Camerman, A., Luo, Y. G., Brayer, G. D., Camerman, N. (1995). Crystal and molecular-structure of paclitaxel (taxol). *Proceedings of the National Academy of Sciences of the United States of America* 92, 6920.
69. Mathew, A. E., Mejillano, M. R., Nath, J. P., Himes, R. H., Stella, V. J. (1992). Synthesis and evaluation of some water-soluble prodrugs and derivatives of taxol with antitumor-activity. *Journal of Medicinal Chemistry* 35, 145.
70. Magri, N. F., Kingston, D. G. I., Jitrangsri, C., Piccariello, T. (1986). Modified taxols. 3. Preparation and acylation of baccatin-III. *The Journal of Organic Chemistry* 51, 3239.
71. Moore, D. R., Cheng, M., Lobkovsky, E. B., Coates, G. W. (2003). Mechanism of the alternating copolymerization of epoxides and CO<sub>2</sub> using beta-diiminate zinc catalysts: evidence for a bimetallic epoxide enchainment. *Journal of the American Chemical Society* 125, 11911.
72. Cheng, M., Moore, D. R., Reczek, J. J., Chamberlain, B. M., Lobkovsky, E. B., Coates, G. W. (2001). Single-site beta-diiminate zinc catalysts for the alternating copolymerization of CO<sub>2</sub> and epoxides: catalyst synthesis and unprecedented polymerization activity. *Journal of the American Chemical Society* 123, 8738.
73. <http://www.doxil.com/doxil-supply-shortage>.
74. <http://www.doxil.com/ovarian-cancer/hand-foot-syndrome>.
75. Lorusso, D., Di Stefano, A., Carone, V., Fagotti, A., Pisconti, S., Scambia, G. (2007). Pegylated liposomal doxorubicin-related palmar-plantar erythrodysesthesia ('hand-foot' syndrome). *Annals of Oncology* 18, 1159.
76. Yoo, H. S., Park, T. G. (2001). Biodegradable polymeric micelles composed of doxorubicin conjugated PLGA-PEG block copolymer. *Journal of Controlled Release* 70, 63.
77. Missirlis, D., Kawamura, R., Tirelli, N., Hubbell, J. A. (2006). Doxorubicin encapsulation and diffusional release from stable, polymeric, hydrogel nanoparticles. *European Journal of Pharmaceutical Sciences* 29, 120.
78. Altreuter, D. H., Dordick, J. S., Clark, D. S. (2002). Nonaqueous biocatalytic synthesis of new cytotoxic doxorubicin derivatives: exploiting unexpected differences in the regioselectivity of salt-activated and solubilized subtilisin. *Journal of the American Chemical Society* 124, 1871.
79. Yoo, H. S., Oh, J. E., Lee, K. H., Park, T. G. (1999). Biodegradable nanoparticles containing doxorubicin-PLGA conjugate for sustained release. *Pharmaceutical Research* 16, 1114.
80. Nishiyama, N., Kataoka, K. (2006). Nanostructured devices based on block copolymer assemblies for drug delivery: designing structures for enhanced drug function. *Advances in Polymer Science* 193, 67.
81. Greenfield, R. S., Kaneko, T., Daus, A., Edson, M. A., Fitzgerald, K. A., Olech, L. J., Grattan, J. A., Spitalny, G. L., Braslawsky, G. R. (1990). Evaluation in vitro of adriamycin immunoconjugates synthesized using an acid-sensitive hydrazone linker. *Cancer Research* 50, 6600.
82. Kaneko, T., Willner, D., Monkovic, I., Knipe, J. O., Braslawsky, G. R., Greenfield, R. S., Vyas, D. M. (1991). New hydrazone derivatives of adriamycin and their

- immunoconjugates: a correlation between acid stability and cytotoxicity. *Bioconjugate Chemistry* 2, 133.
83. Ulbrich, K., Subr, V. (2004). Polymeric anticancer drugs with pH-controlled activation. *Advanced Drug Delivery Reviews* 56, 1023.
84. Florent, J. C., Monneret, C. (2008). Doxorubicin conjugates for selective delivery to tumors. *Anthracycline Chemistry and Biology II: Mode of Action, Clinical Aspects and New Drugs* 283, 99.
85. Farokhzad, O. C., Cheng, J., Teply, B. A., Sherifi, I., Jon, S., Kantoff, P. W., Richie, J. P., Langer, R. (2006). Targeted nanoparticle-aptamer bioconjugates for cancer chemotherapy *in vivo*. *Proceedings of the National Academy of Sciences of the United States of America* 103, 6315.
86. Caliceti, P., Veronese, F. M. (2003). Pharmacokinetic and biodistribution properties of poly(ethylene glycol)-protein conjugates. *Advanced Drug Delivery Reviews* 55, 1261.
87. Pierri, E., Avgoustakis, K. (2005). Poly(lactide)-poly(ethylene glycol) micelles as a carrier for griseofulvin. *Journal of Biomedical Materials Research. Part A* 75A, 639.
88. Tuerk, C., Gold, L. (1990). Systematic evolution of ligands by exponential enrichment: RNA ligands to bacteriophage-T4 DNA-polymerase. *Science* 249, 505.
89. Ellington, A. D., Szostak, J. W. (1992). Selection *in vitro* of single-stranded-DNA molecules that fold into specific ligand-binding structures. *Nature* 355, 850.
90. Farokhzad, O. C., Jon, S. Y., Khadelmhosseini, A., Tran, T. N. T., LaVan, D. A., Langer, R. (2004). Nanoparticle-aptamer bioconjugates: a new approach for targeting prostate cancer cells. *Cancer Research* 64, 7668.
91. Keefe, A. D., Pai, S., Ellington, A. (2010). Aptamers as therapeutics. *Nature Reviews Drug Discovery* 9, 537.
92. Nimjee, S. M., Rusconi, C. P., Sullenger, B. A. (2005). Aptamers: an emerging class of therapeutics. *Annual Review of Medicine* 56, 555.
93. Cao, Z. H., Tong, R., Mishra, A., Xu, W. C., Wong, G. C. L., Cheng, J. J., Lu, Y. (2009). Reversible cell-specific drug delivery with aptamer-functionalized liposomes. *Angewandte Chemie (International edition)* 48, 6494.
94. Lupold, S. E., Hicke, B. J., Lin, Y., Coffey, D. S. (2002). Identification and characterization of nuclease-stabilized RNA molecules that bind human prostate cancer cells via the prostate-specific membrane antigen. *Cancer Research* 62, 4029.
95. Chaney, E. J., Tang, L., Tong, R., Cheng, J. J., Boppart, S. A. (2010). Lymphatic biodistribution of polylactide nanoparticles. *Molecular Imaging* 9, 153.
96. Chan, J. M., Zhang, L. F., Tong, R., Ghosh, D., Gao, W. W., Liao, G., Yuet, K. P., Gray, D., Rhee, J. W., Cheng, J. J., Golomb, G., Libby, P., Langer, R., Farokhzad, O. C. (2010). Spatiotemporal controlled delivery of nanoparticles to injured vasculature. *Proceedings of the National Academy of Sciences of the United States of America* 107, 2213.
97. Kaplan, B., Meier-Kriesche, H. U. (2004). Renal transplantation: a half century of success and the long road ahead. *Journal of the American Society of Nephrology* 15, 3270.
98. Wong, W., Venetz, J. P., Tolkoff-Rubin, N., Pascual, M. (2005). Immunosuppressive strategies in kidney transplantation: which role for the calcineurin inhibitors? *Transplantation* 80, 289.
99. Chapman, J. R., Nankivell, B. J. (2006). Nephrotoxicity of ciclosporin A: short-term gain, long-term pain? *Nephrology, Dialysis, Transplantation* 21, 2060.

100. Neto, A. B., Haapalainen, E., Ferreira, R., Feo, C. F., Misiako, E. P., Vennarecci, G., Porcu, A., Dib, S. A., Goldenberg, S., Gomes, P. O., Nigro, A. T. (1999). Metabolic and ultrastructural effects of cyclosporin A on pancreatic islets. *Transplant International* 12, 208.
101. Azzi, J., Tang, L., Moore, R., Tong, R., El Haddad, N., Akiyoshi, T., Mfarrej, B., Yang, S. M., Jurewicz, M., Ichimura, T., Lindeman, N., Cheng, J. J., Abdi, R. (2010). Polylactide-cyclosporin A nanoparticles for targeted immunosuppression. *The FASEB Journal* 24, 3927.
102. Rieth, L. R., Moore, D. R., Lobkovsky, E. B., Coates, G. W. (2002). Single-site beta-diiminate zinc catalysts for the ring-opening polymerization of beta-butyrolactone and beta-valerolactone to poly(3-hydroxyalkanoates). *Journal of the American Chemical Society* 124, 15239.
103. Sharp, P. A., Langer, R. (2011). Promoting convergence in biomedical science. *Science* 333, 527.
104. Wong, C., Stylianopoulos, T., Cui, J. A., Martin, J., Chauhan, V. P., Jiang, W., Popovic, Z., Jain, R. K., Bawendi, M. G., Fukumura, D. (2011). Multistage nanoparticle delivery system for deep penetration into tumor tissue. *Proceedings of the National Academy of Sciences of the United States of America* 108, 2426.
105. Sugahara, K. N., Teesalu, T., Karmali, P. P., Kotamraju, V. R., Agemy, L., Greenwald, D. R., Ruoslahti, E. (2010). Coadministration of a tumor-penetrating peptide enhances the efficacy of cancer drugs. *Science* 328, 1031.
106. Jain, R. K., Stylianopoulos, T. (2010). Delivering nanomedicine to solid tumors. *Nature Reviews Clinical Oncology* 7, 653.
107. Torchilin, V. P. (2006). Multifunctional nanocarriers. *Advanced Drug Delivery Reviews* 58, 1532.
108. Sutton, D., Nasongkla, N., Blanco, E., Gao, J. M. (2007). Functionalized micellar systems for cancer targeted drug delivery. *Pharmaceutical Research* 24, 1029.
109. Chaffer, C. L., Weinberg, R. A. (2011). A perspective on cancer cell metastasis. *Science* 331, 1559.
110. Hanahan, D., Weinberg, Robert A. (2011). Hallmarks of cancer: the next generation. *Cell* 144, 646.

